ANALYTICAL AVERAGING METHOD IN SCATTERING OF LIGHT BY ENSEMBLES OF NONSPHERICAL AEROSOLS

D. N. Nicolae, C. Talianu, M. Ciobanu[*], C. Radu, V. Babin, C. P. Cristescu[a]

National Institute for Optoelectronics, Bucharest-Magurele, Romania
[a]"Politehnica" University, Bucharest, Romania

In many fields of science and engineering, accurate information about light scattering properties of small nonspherical particles are necessary. In the so-called resonance region of particle size parameters, numerical methods for computing nonspherical scattering must be based on directly solving Maxwell's equations, because Rayleigh and geometric optics approximations are inapplicable. In this paper, we review the status of Waterman's *T*-matrix approach and we present some results obtained by computing orientationally-averaged light scattering characteristics for ensembles of nonspherical particles.

1. Introduction

The matrix method is an exact method based on the assumption that both the incident and the scattered fields can be expanded in vector spherical functions. In this sense, it can be considered as an extension to the Mie theory. This method was introduced by Waterman [3] in 1971 for an homogenous particle and then generalized for nonspherical particle clusters by Peterson and Strom [4] in 1974. The advantages of this method reside in the fact it is an exact and rapid method, and it can be applied to particles having the dimensional parameter < 125. This means that a *T*-Matrix + Geometrical Optics combination could cover the entire dimensional spectrum for particles with rotational symmetry.

To use this method, we define some important parameters for the scattering of light on nonspherical particles:

➢ phase asymmetry parameter, defined as:

$$g = \langle \cos\theta \rangle = \frac{1}{2}\int_{-1}^{1} d(\cos\theta) a_1(\theta)\cos\theta \tag{1}$$

It is positive for particles which scatter the light predominantly forward, negative for those which scatter the light predominantly backward, and zero for symmetrical phase functions.

➢ the assembly average of absorption cross section per particle, defined as the difference between corresponding transversal extinction cross section and scattering cross section:

$$C_{abs} = C_{ext} - C_{sca} \tag{2}$$

➢ the albedo of simple scattering, defined as the probability for an incident photon on the elemental scattering volume to be present at the end of the process, and which satisfies the relationship:

$$\overline{w} = \frac{C_{sca}}{C_{ext}} \tag{3}$$

---

[*] Corresponding author: mircea@inoe.inoe.ro

➢   the irradiance of the scattered radiation, as function of the incident radiation, average cross section of one particle, the density of particles per unit volume and the remote distance, and which is determined via the amplitude matrix:

$$I^{sca} = \frac{C_{sca} n_0 dv}{4\pi R^2} F(\theta) I^{inc} \tag{4}$$

The computation of the transfer matrix T for a particle involves expanding the incident and scattered field in vector spherical functions [1].

$$\vec{E}^{inc}(\vec{R}) = \sum_{n=1}^{\infty} \sum_{m=-n}^{n} \left[a_{mn} RgM_{mn}(k\vec{R}) + b_{mn} RgN_{mn}(k\vec{R}) \right] \tag{5}$$

$$\vec{E}^{sca}(\vec{R}) = \sum_{n=1}^{\infty} \sum_{m=-n}^{n} \left[p_{mn} M_{mn}(k\vec{R}) + q_{mn} N_{mn}(k\vec{R}) \right], R > r_0 \tag{6}$$

Due to the linearity of Maxwell's equations and of the boundary conditions, the relation between the coefficients p_{mn} si q_{mn} of the scattered field and the a_{mn} si b_{mn} of the incident field is linear and is given by a transfer matrix (the T matrix)

$$\begin{bmatrix} p \\ q \end{bmatrix} = T \begin{bmatrix} a \\ b \end{bmatrix} = \begin{bmatrix} T^{11} & T^{12} \\ T^{21} & T^{22} \end{bmatrix} \begin{bmatrix} a \\ b \end{bmatrix} \tag{7}$$

having the following characteristics:
-    the matrix elements are independent of the incident and scattered field, so once calculated they can be used for any incident or scattered angle;
-    the matrix elements depend only on the shape, dimensional parameter and refractive index of the scatterer, as well as on its orientation in the coordinate system;
-    the mathematical functions from the matrix expression are well-known, so their computation is very easy, and the analytical average of the scattered light on a randomly oriented particle assembly becomes possible.

2. Experimental

2.1 Theory

In order to compute the T matrix in the natural frame we use the extended boundary condition method (EBCM) developed by Waterman [2] for homogenous particles. In addition to the expansion of the incident and scattered field, the internal field is also expanded in vector spherical functions [7]:

$$\vec{E}^{int}(\vec{R}) = \sum_{n=1}^{\infty} \sum_{m=-n}^{n} \left[c_{mn} RgM_{mn}(n_{rel} k\vec{R}) + d_{mn} RgN_{mn}(n_{rel} k\vec{R}) \right] \tag{8}$$

The relation between the expansion coefficients of the incident and internal fields is linear and is given by:

$$\begin{bmatrix} a \\ b \end{bmatrix} = \begin{bmatrix} Q^{11} & Q^{12} \\ Q^{21} & Q^{22} \end{bmatrix} \begin{bmatrix} c \\ d \end{bmatrix} \tag{9}$$

where the elements of the Q matrix are two-dimensional integrals which must be numerically evaluated over the particle surface and depend on the particle size, shape, refractive index, and orientation. So:

$$T = -RgQ[Q]^{-1} \tag{10}$$

where, again, the elements of Q and RgQ are two-dimensional integrals over the particle surface, which, in the case of rotational - symmetric particles become:

$$\int_0^\pi d\theta \sin \theta f(\theta), \tag{11}$$

where θ is the polar angle. These intervals are evaluated using the Gauss method:

$$\int_0^\pi d\theta \sin \theta f(\theta) \approx \sum w_k \sin \theta_k f(\theta_k) \tag{12}$$

where θ_k and w_k are discrete points, and weights on the interval $[0,\pi]$.

Although the T matrix is infinite, a finite truncated value must be chosen in practical computer calculations. The convergence dimension for the T matrix is obtained by increasing a computational parameter, n_{max}, in unitary steps until both the optical cross sections and expansion coefficients are converging with some accuracy.

Further, one can average over the nonspherical, randomly oriented particles. The scattering matrix elements can be expanded using the generalized spherical functions $P_{pq}^s(\cos\theta)$.

$$F_{pq}^C(\theta) = \sum_{s=\max(|p|,|q|)}^\infty g_{pq}^s P_{pq}^s(\cos\theta) \quad p,q = 2,0,-0,-2 \tag{13}$$

In the standard (I, Q, U, V) polarization representation [6], the matrix have a block-diagonal form:

$$F(\theta) = \begin{bmatrix} F_{11}(\theta) & F_{12}(\theta) & 0 & 0 \\ F_{12}(\theta) & F_{22}(\theta) & 0 & 0 \\ 0 & 0 & F_{33}(\theta) & F_{34}(\theta) \\ 0 & 0 & -F_{34}(\theta) & F_{44}(\theta) \end{bmatrix} \tag{14}$$

where the matrix elements are infinite series:

$$F_{11}(\theta) = \sum_{s=0}^\infty a_1^s P_{00}^s(\cos\theta)$$

$$F_{22}(\theta) + F_{33}(\theta) = \sum_{s=0}^\infty \left(a_2^s(\theta) + a_3^s(\theta)\right) P_{22}^s(\cos\theta)$$

$$F_{22}(\theta) - F_{33}(\theta) = \sum_{s=0}^\infty \left(a_2^s(\theta) - a_3^s(\theta)\right) P_{2-2}^s(\cos\theta)$$

$$F_{44}(\theta) = \sum_{s=0}^\infty a_4^s P_{00}^s(\cos\theta)$$

$$F_{12}(\theta) = \sum_{s=0}^\infty b_1^s P_{02}^s(\cos\theta)$$

$$F_{34}(\theta) = \sum_{s=0}^\infty b_2^s P_{02}^s(\cos\theta)$$

$$a_1^s = g_{00}^s + g_{0-0}^s$$
$$a_2^s = g_{22}^s + g_{2-2}^s$$
$$a_3^s = g_{22}^s - g_{2-2}^s$$
$$a_4^s = g_{00}^s - g_{0-0}^s$$
$$b_1^s = 2\,\mathrm{Re}\,g_{02}^s$$
$$b_2^s = 2\,\mathrm{Im}\,g_{02}^s$$

with:

$$\tag{15}$$

In the most frequent case in the atmosphere - randomly oriented particles - the orientation distribution function $P(\alpha, \beta, \gamma)$ equals $\left(8\pi^2\right)^{-1}$. In this case we obtain the T matrix for the average orientation [10]:

$$\left\langle {}^2T_{mnm'n'}^{ij}\right\rangle = \frac{1}{2n+1}\delta_{mm'}\cdot\delta_{nn'}\sum_{m_1=-n}^{n}{}^1T_{m_1nm_1n}^{ij}\,,\quad i,j=1,2 \tag{16}$$

Consequently, for randomly oriented particles, we can calculate the orientation averaged extinction cross section:

$$\left\langle C_{ext}\right\rangle = \frac{2\pi}{k}\,\mathrm{Im}\!\left[\left\langle S_{\vartheta\vartheta}(\vec{n},\vec{n})\right\rangle + \left\langle S_{\varphi\varphi}(\vec{n},\vec{n})\right\rangle\right] = -\frac{2\pi}{k^2}\,\mathrm{Re}\sum_{n=1}^{\infty}\sum_{m=-n}^{n}\left[{}^1T_{mnmn}^{11}+{}^1T_{mnmn}^{22}\right] \tag{17}$$

or, after the scattering:

$$\left\langle C_{sca}\right\rangle = \frac{2\pi}{k^2}\sum_{n=1}^{\infty}\sum_{n'=1}^{\infty}\sum_{m=-n}^{n}\sum_{m'=-n'}^{n'}\sum_{i=1}^{2}\sum_{j=1}^{2}\left|{}^1T_{mnm'n'}^{ij}\right|^2 \tag{18}$$

So, instead of numerically integrating the optical cross section and the matrix elements for various orientation, we compute the T matrix for a single particle, and then introduce the result in the analytical average procedure above. This method, developed by M. Mishchenko et al. [8], reduces drastically the computer time.

2.2 Modelling

The model is applied to particles with rotational symmetry, which are frequently encountered in the atmosphere. In order to characterize the size and dimension related to the specific dimensional parameters, we used the radius of a sphere having the same volume as that of a given particle.
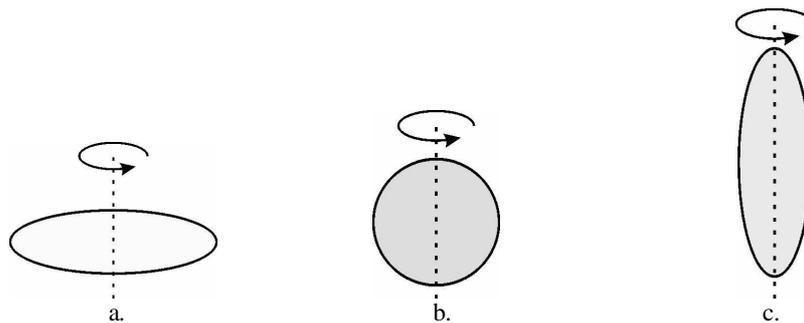
Fig. 1. Spheroids with varying axial ratios, a. oblate spheroid; b. sphere; c. prolate spheroid.

Taking this into account, we average over the dimension of the particles the transversal optical cross section and the coefficients in the development (15). For this, we numerically evaluate the integrals:

$$C_{sca} = \int_{r_1}^{r_2} dr\, n(r)\, C_{sca}(r) \tag{19}$$

$$C_{ext} = \int_{r_1}^{r_2} dr\, n(r)\, C_{ext}(r) \tag{20}$$

$$a_i^s = \frac{1}{C_{sca}} \int_{r_1}^{r_2} dr n(r) C_{sca}(r) a_i^s(r) \qquad i = 1,...,4 \tag{21}$$

$$b_i^s = \frac{1}{C_{sca}} \int_{r_1}^{r_2} dr n(r) C_{sca}(r) b_i^s(r) \qquad i = 1,...,4 \tag{22}$$

and we model the dimensional distribution of aerosols using the specific functions: the gamma distribution, the modified gamma distribution, the log-normal distribution, or the power distribution. M. Mishchenko et. al. [9] realized a code in order to evaluate the series coefficients (a_1^s, a_2^s, a_3^s, a_4^s, b_1^s, b_2^s), the T matrix elements (F_{11}, F_{22}, F_{33}, F_{44}, F_{12}, F_{34}), the mean over the orientation of the extinction cross section (*Cext*) and scattering (*Csca*), of the albedo (*w*) and of the asymmetry parameter of the phase function ($<\cos\theta>$). The authors of this paper have used this code, modified as to calculate (*Isca/Iinc*). Several runs were made, for different kind of particles, considering the power law:

$$n(R) = \frac{2R_{min}^2 R_{max}^2}{R_{max}^2 - R_{min}^2} \cdot \frac{1}{R^3} \qquad R \in \left[R_{min}, R_{max}\right] \tag{23}$$

In the runs, we considered a monochromatic electromagnetic (laser) radiation with $\lambda = 0.532\mu m$ (green) which scatters on an assembly of monarch with the index of refraction $n_{refr} = 1.57 + 0.53 \cdot i$, in colloidal suspension in air (of unitary refractive index). The computer calculations were done for volume-equivalent spheroidal and spherical particles, for two size ranges: 'large' particles ($R > 1\mu m$) and 'small' particles ($R < 1\mu m$), considering in parallel the prolate and the oblate spheroids to evidence the influence of the non-sphericity and the influence of the particle size on the scattered field. In all of the cases considered, the absolute accuracy of computing the expansion coefficients was $\Delta = 10^{-3}$.

For the power law size distribution, the effective equal-volume-sphere-radius R_{eff} [5] is equal to the equal-volume-sphere-radius of the monodisperse spheroids:

$$R_{eff} = \frac{R_{max} - R_{min}}{\ln\left(\frac{R_{max}}{R_{min}}\right)} \tag{24}$$

and the effective variance is:

$$V_{eff} = \frac{R_{max} + R_{min}}{2(R_{max} - R_{min})} \cdot \ln\left(\frac{R_{max}}{R_{min}}\right) - 1 \tag{25}$$

By taking into account particles with values of V_{eff} smaller but close to the unity, we have a moderately wide size distribution. In our computations we considered the following cases:

Table 1. Study cases.

Particle type	R_{min}	R_{max}	R_{eff}	V_{eff}	Axial ratio a/b
prolate big spheroids	0.5	1.5	0.9102	0.0986	0.6; 0.7; 0.8;1.0
oblate big spheroids	0.5	1.5	0.9102	0.0986	1.7; 1.4; 1.2; 1.0
prolate small spheroids	0.2	0.6	0.3641	0.0986	0.6; 0.7; 0.8;1.0
oblate small spheroids	0.2	0.6	0.3641	0.0986	1.7; 1.4; 1.2; 1.0

3. Results

In Fig. 2 are shown for comparison the results obtained in computation of the scattering matrix elements for "big" particles in two cases: prolate (a) and oblate (b) spheroids. The black line is associated with spherical particles of the same R_{eff} and V_{eff} (case: a/b = 1).

In Fig. 3 the same analysis is shown, but for "small" polydisperse particles, also prolate, oblate and spherical. Some calculations for the angular dependence of the scattered intensity were done by considering the particles concentration in an elementary volume equal to 10^{-3} mg/m^3.
The scattered – incident intensity ratio for each case is plotted in Fig. 4.

Other computation results, as the values for the optical extinction and scattering cross section for each case, the single-scattering albedo and the asymmetry parameter of the phase function, are given in Table 2.
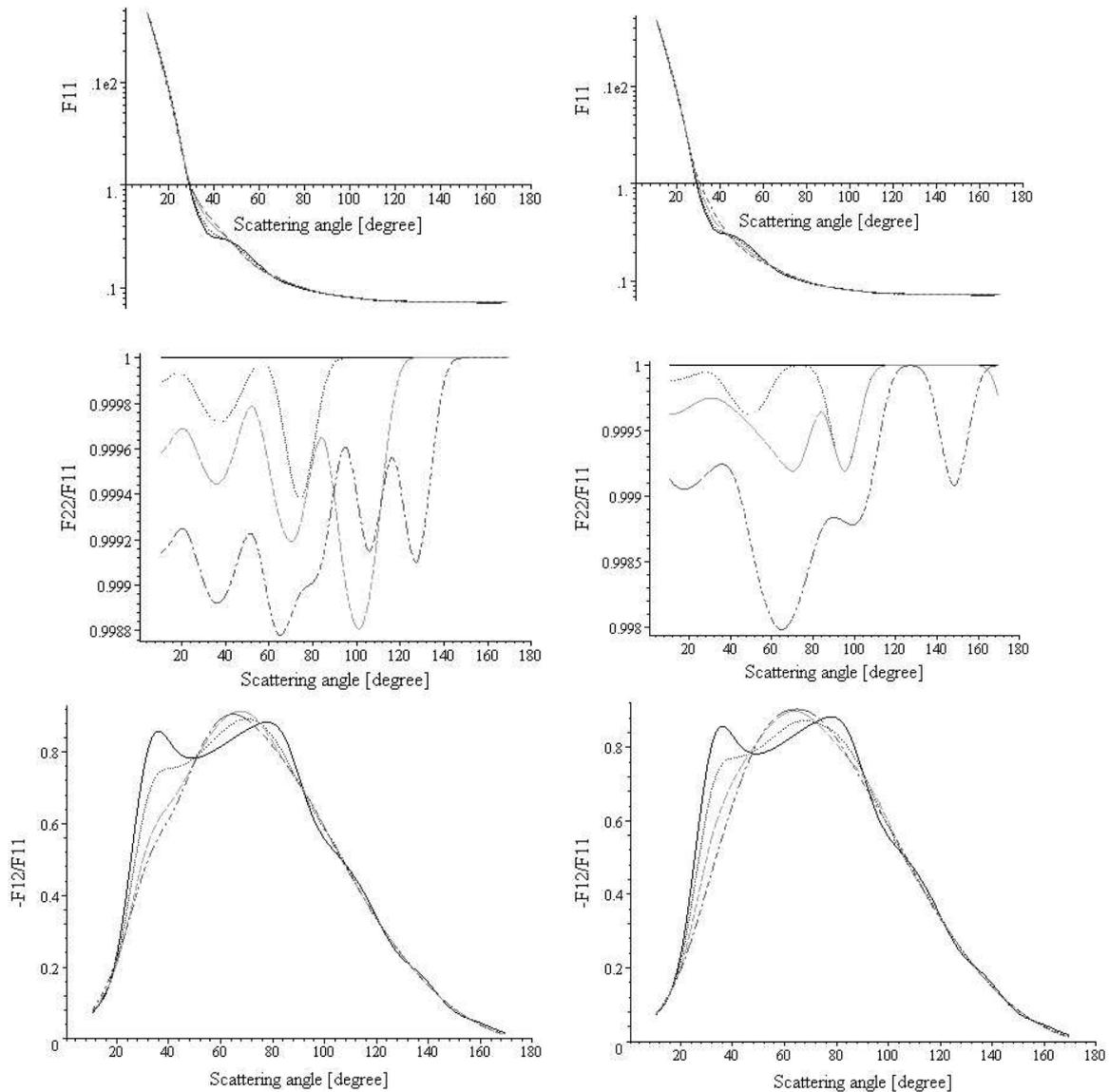
Fig. 2. Elements of the scattering matrix vs. scattering angle for "big" smoke particles (n_{Re} = 1.57, n_{Im} = 0.53) investigated with laser radiation (λ = 0.532 μm) a. prolate spheroids: a/b = 0.6 (dash - dot line), 0.7 (dash line), 0.8 (dot line), 1 (solid line) b. oblate spheroids: a/b = 1.7 (dash-dot line), 1.4 (dash line), 1.2 (dot line), 1 (solid line).
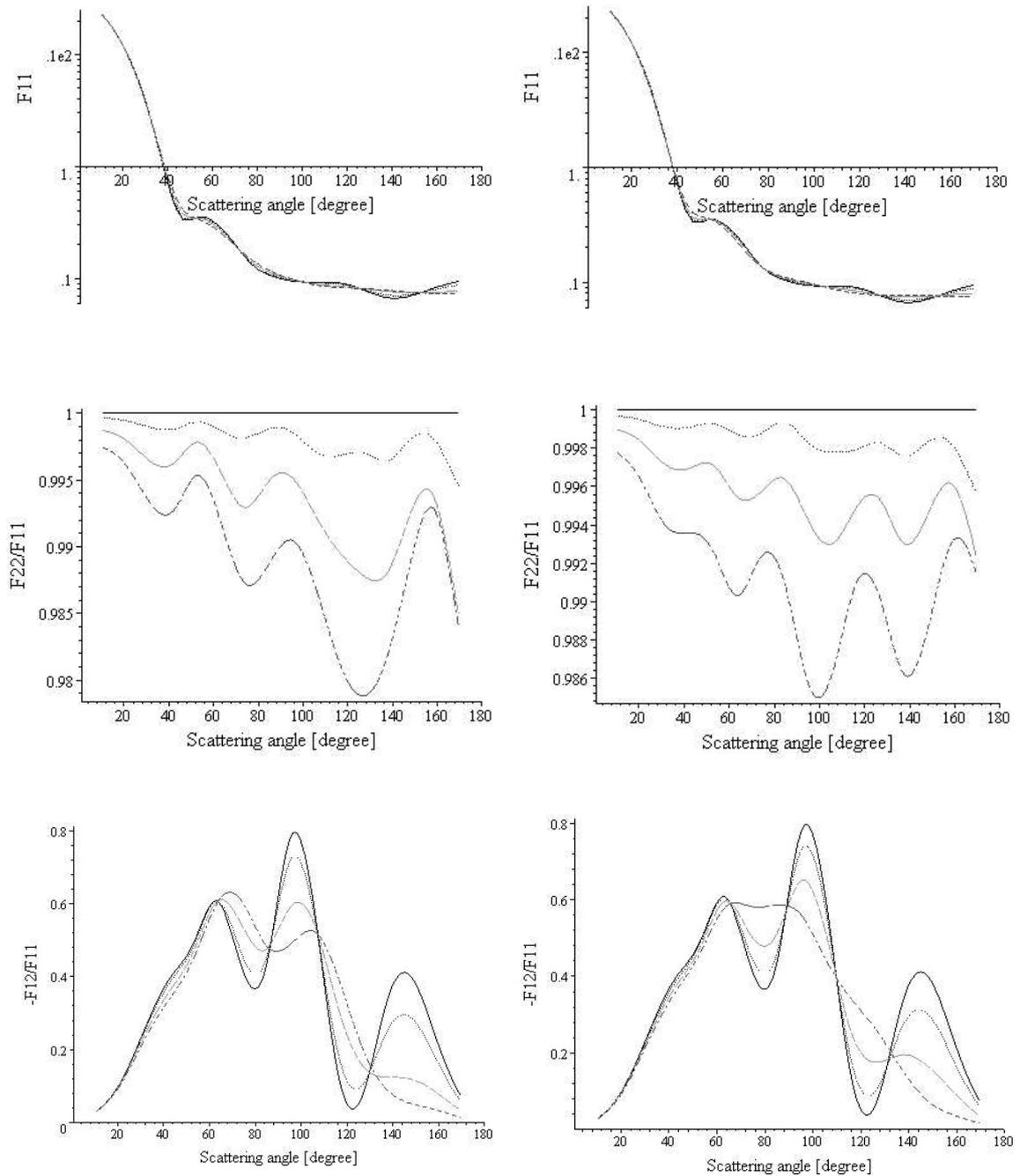
Fig. 3 Elements of the scattering matrix vs. scattering angle for "small" smoke particles ($n_{Re} = 1.57$, $n_{Im} = 0.53$) investigated with laser radiation ($\lambda = 0.532$ μm): a. oblate spheroids: a/b = 1.7 (dash-dot line), 1.4 (dash line), 1.2 (dot line), 1 (solid line), b. oblate spheroids: a/b = 1.7 (dash-dot line), 1.4 (dash line), 1.2 (dot line), 1 (solid line).
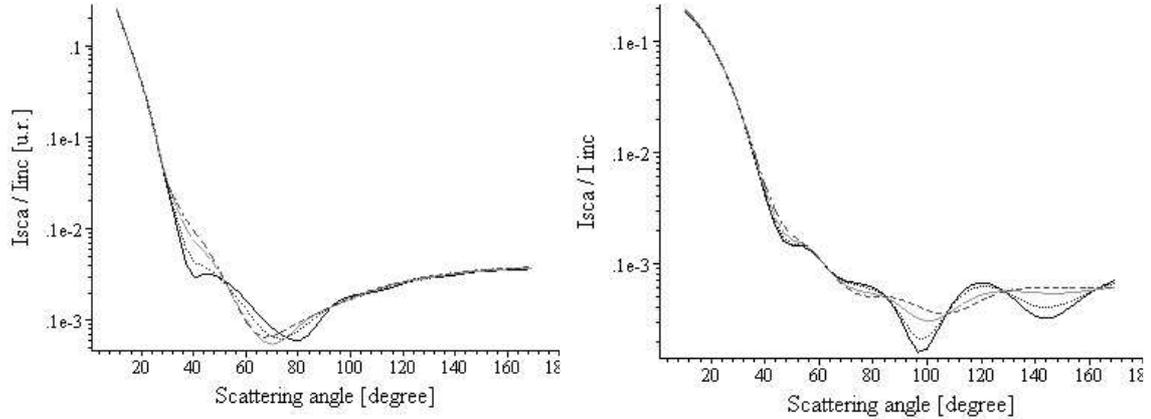
Fig. 4 Scattering and incident intensity ratio vs. scattering angle for prolate smoke particles
($n_{Re} = 1.57$, $n_{Im} = 0.53$) investigated with laser radiation ($\lambda = 0.532\,\mu m$): a. "big" particles;
b. "small" particles

Table 2. Scattering parameters for prolate smoke particles.

a/b	Optical extinction cross section [μm^2]		Optical scattering cross section [μm^2]		Single-scattering albedo		Asymmetry parameter of the phase function	
Prolate	"Big" spheroids	"Small" spheroids	"Big" spheroids	"Small" spheroids	"Big" spheroids	"Small" spheroids	"Big" spheroids	"Small" spheroids
0.6	7.63660	1.34148	3.97685	0.635799	0.520762	0.473953	0.895174	0.848856
0.7	7.48985	1.31677	3.89991	0.622123	0.520692	0.472462	0.895399	0.849041
0.8	7.38583	1.29944	3.84502	0.612352	0.520594	0.471242	0.895542	0.849196
1.0	7.34576	1.29284	3.82376	0.608560	0.520539	0.470715	0.895590	0.849254
Oblate	"Big" spheroids	"Small" spheroids	"Big" spheroids	"Small" spheroids	"Big" spheroids	"Small" spheroids	"Big" spheroids	"Small" spheroids
1.7	7.69898	1.35146	4.01466	0.642997	0.521453	0.475779	0.895309	0.850484
1.4	7.48445	1.31592	3.89831	0.622028	0.520855	0.472693	0.895466	0.849566
1.2	7.38575	1.29947	3.84518	0.612414	0.520621	0.471280	0.895552	0.849290
1.0	7.34576	1.29284	3.82376	0.608560	0.520539	0.470715	0.895590	0.849254

4. Discussion

Concerning the matrix element associated with the scattered intensity (F_{11}), the angular variation is the same for both prolate and oblate particles having the same dimensions, and relatively close to the polydisperse particles. Note that in Figs. 1 and 2 the scale of F_{11} is logarithmic. We can observe that the profile of the graph is less pronounced in the case of large particles than in the case of small particles, in good agreement with the Mie theory for spherical particles. Generally, we see a strong forward scattering, the other directions being less represented, because the absorption cross section for this kind of particles (having a relatively large imaginary part of the refractive index) is large, especially for nonspherical particles (see Table 2).

Despite the fact that for spherical particles $F_{22}/F_{11} = 1$, in the case of spheroids this ratio depends on the asphericity, as we can see from Figs. 2 and 3, where the three curves corresponding to different axial ratios are different. The deviation from unity is lesser for oblate spheroids than for prolates having the same dimensions and increases with the increase of the asymmetry ratio (a/b).

The linear polarization, associated to the ratio ($-F_{12}/F_{11}$), have a similar behavior for prolate and oblate spheroids, as in the case of F_{11}.

The scattered and incident irradiance ratio shows a similar behavior in all cases, but the forward direction is encouraged, while the normal to incident radiation direction scattering is less pronounced. A small increase in the radiation backscattered is also observed. Likewise, we observe the maximum are less pronounced as the sphericity deviation becomes larger. For equalsize particles, the difference between prolate and oblate is not significant, but we can observe that for larger particles the scattering angle dependence of the ratio is very different, both in profile and in value, for large particles and for small particles. In the case of large particles, the forward and backward directions maxima, and the minima for the normal directions are more pronounced. Likewise, we have to note that for nonspherical particles, the backscattering is weaker than for spherical ones, a fact resulted from the profile near the 180° scattering angle.

Concerning the extinction and scattering cross sections, as well as for the albedo for simple scattering, from Table 2 we see that their values are greater the greater the sphericity deviation is. Nevertheless, if the sphericity deviation is less or moderate, the differences from the polydisperse particles case are negligible.

5. Conclusions

By computer calculations, we have found that the angular behavior of the elements of the scattering matrix for nonspherical particles differs significantly from that of the scattering matrix for equivalent spherical particles. In particular, by comparison to the spherical particles:
- the size distribution of spheroids exhibits stronger side scattering and weaker
  backscattering;
- the ratio F_{22}/F_{11} deviates from the unity;
- the element F_{33} differs from the element F_{44} of the scattering matrix (in general is greater);
- the ratios F_{22}/F_{11}, F_{33}/F_{11} and F_{34}/F_{11} can differ substantially for prolate and oblate spheroids of the same aspect ratio, thus they can be indicators of particle shape - for oblate spheroids, the ratio F_{22}/F_{11} is closer to the unity than for prolate spheroids, and F_{33} is closer to F_{44};
- the angular pattern of F_{11}, intensity and linear polarization ($-F_{12}/F_{11}$) are similar, so they cannot give a valid information about the shape of the particles, although with increasing asphericity of oblate and prolate spheroids the profile of linear polarization curves becomes be more smooth;
- the scattering and extinction cross sections, as well as the single-scattering albedo and the asymmetry parameter of the phase-function are very similar for the moderately aspherical spheroids and spherical particles;
- in general, all the light-scattering characteristics are more shape-dependent for larger particles.

References

[1] I. M. Gelfand, R. A. Minlos, Z. Ya. Shapiro, Representations of the Rotation and Lorentz Groups and Their Applications, Pergamon Press, Oxford, 1963.
[2] P. C. Waterman, Proc. IEEE, **53**, 805 (1965).
[3] P. C.Waterman, Symmetry, unitarity, and geometry in electromagnetic scattering, Phys. Rev. D, **3**, 825 (1971).
[4] B. Peterson, S. Strom, T matrix for electromagnetic scattering from multilayered scatterers, Phys. Rev. D, **10**, 2670 (1974).
[5] J. E. Hansen, L. D. Travis, Space Sci. Rev. **16**, 527 (1974).
[6] C. F. Bohren, D. R. Huffman, Absorption and Scattering of Light by Small Particles, Wiley, New York, 1983.
[7] D. A. Varshalovich, A. N. Moskalev, V. K. Khersonskii, Quantum Theory of Angular Momentum, World Scientific, Singapore, 1988.
[8] M. I. Mishchenko, Light scattering by randomly oriented axially symmetric particles, J. Opt.

Soc. Am. A **8**(6), 871 (1991).

[9] M. I. Mishchenko, L. D. Travis, Capabilities and limitations of a current Fortran implementation of the T-matrix method for randomly oriented, rotationally symmetric scatterers, J. Quant. Spectrosc. Radiat. Transfer **60**(3), 309 (1998).

[10] M. I. Mishchenko, J. W. Hovenier, L. D. Travis, Light Scattering by Nonspherical Particles. Theory, Measurements, and Applications, Academic Press, San Diego, 152, 2000.